

Specification of QSPECT program

- Reconstruction is carried out according to OSEM with attenuation correction. Projection data should be geometric-mean (GM) for parallel-beam.
- Transmission-dependent convolution subtraction (TDCS) method has been employed as scatter correction. Attenuation-to-scatter fraction tables are presented for ^{99m}Tc , ^{201}Tl , ^{123}I isotopes. The table for ^{123}I includes collimator penetration process determined empirically for various collimators from various manufacturers.
- μ map from TCT (or edge-detection for brain).
- Mmap generated from X-ray CT ma also be of use
- Pixel counts are presented in units of Bq/mL. (BCF (Bq Calibration Factor) needs to be defined prior to use)

Pixel counts (Bq/mL) are independent of

- Scan duration
- The number of heads
- Kinds of collimator
- Pixel size (64x64 or 128x128 etc)
- Radioisotope
- Manufacturer
- etc
- JAVA interface, with C code as the foundation.
- R/W format: Dicom, Analyze, and Dr.View.
- Runs on Windows (XP) with JAVA 1.4.1 or more. CPU 3GHz. Memory 512 MB. Disk space>30MB. Display > XGA (1024x768).
- Emission Projection File should be
 - Uniformity corrected.
 - Parallel-beam (need to be converted to parallel-beam equivalent if acquired by fanbeam collimator)
 - File format should be Dicom, Analyze or Dr.View

1. Input Files

a) Projection file

File name should have 18 characters as a general rule. Maximum 23 characters. Our rule is as follows.

File Name : [patient ID]_[date]_[modality]_[type].(ext)
- Patient ID : 7 characters
- Date : 3 characters (ymd : year-month-day)
- Modality : 1 character
- Type: 4 characters (2 characters for acquisition, 2 characters for study)
- Ext : Extension (dcm for DICOM, hdr/img for ANALYZE)

Example)

1234567_44b_s_p1sr.dcm
Patient ID : 1234567
Study date : 11 April 2004
Acquisition equipment : SPECT
Data type : reconstructed static image from 1st static scan data

Data format should be either Dicom, Analyze or Dr.View.

b) Attenuation mu-map file

This program can read mu-map for given radioisotopes. This file should be in Analyze format, and should have units of cm^{-1} . Pixel counts may be approximately 0.15 for ^{99m}Tc in water. Two-dimensional mu-maps should be defined at each slice pixel in the projection data.

The mu-map may also be generated in this program by defining edge of attenuation-uncorrected FBP images. This option may be used for some brain studies.

2. Temporary Files

File format is ANALYZE.

[img-file-name]_UNIMAP: uniform attenuation-map generated by using edge-detection (if mu-map is defined by edge-detection program)

[img-file-name]_Scat: Estimated scatter-component projection

[img-file-name]_Prim: Scatter-corrected projection (with geometric mean typed)

[img-file-name]_ACSC: Reconstructed image with attenuation + scatter correction

[img-file-name]_NoAC: Reconstructed image with no attenuation using FBP

[img-file-name]_UNIMAP_MuAP: Transmission projection calculated from Mu map

3. Output File

Output file name can be defined in the user interface window. Default file name is defined by replacing 18th character with "r". File format is the same as input file format (Dicom, Analyze, Dr.View).

Input file...ex) 1234567_44b_s_ils_.img
 Output file (default) . . . ex) 1234567_44b_s_ilsr.img

4. Parameter Files

def.txt: Default parameters are saved into this file by [File]->[Default]->[Save]. Thickness, Pitch, Iteration, Subset, Camera Rotation, Start Angle, Head-In/Feet-In, Emission Isotope, Transmission Isotope, BCF, TDCS parameter, Threshold(%), Mu-value, cm^{-1}

env.txt: Parameter set by [Settings]->[Options] are save into this file. Data directory, temporary directory etc.

para.txt: Parameter values set on the menu window are saved into this file. Slice Select, Scan Information, OSEM Parameter, etc

QSPECT_000_S_BCF.txt: Bequerrel calibration factor (BCF)

QSPECT_000_S_BCF_Default.txt: BCF defaults

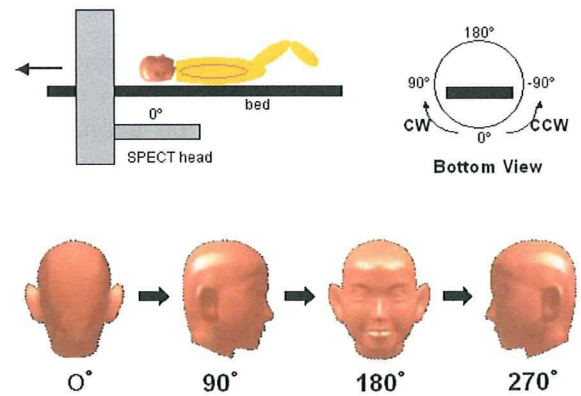
[image-file-name].time :

Number of frames, Acquisition time for each view for each frame, Number of Heads

5. Definition of acquisition setting

QSPECT has an original definition of axis of coordinates. You should set up parameters (camera-rotation, start-angle, subject-position)

so as to show projection as below.



Projection data should be displayed as in this figure in the main menu window. Set three parameters of camera-rotation, start-angle, subject-position, so as to display as this.

	Rotation	Start Angle	Orientation
	CW	0	Head-in
	CW	90	Head-in
	CCW	0	Head-in
	CW	0	Feet-in

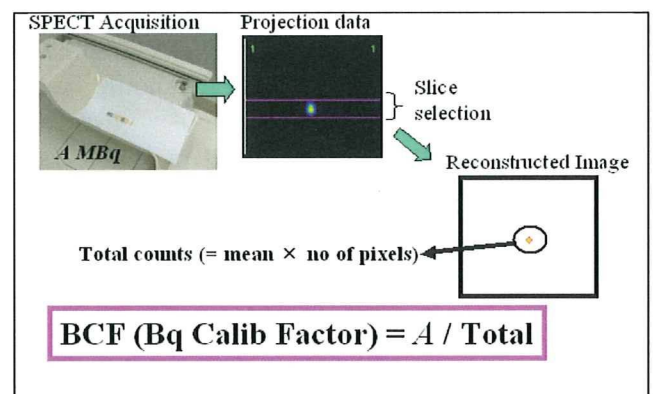
Example of set-up parameters (Rotation, Start Angle, Orientation)

Operation of the program

1. Settings

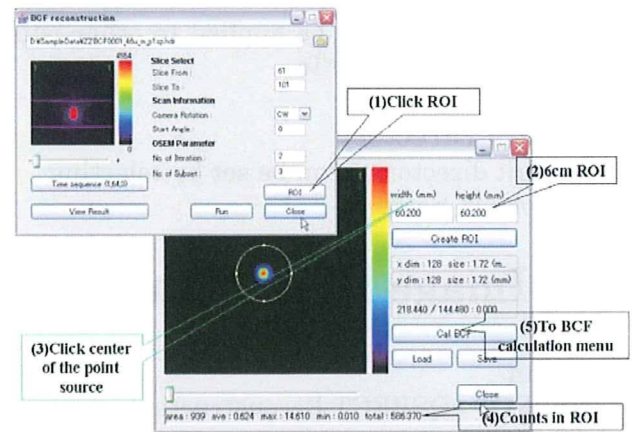
a) BCF (Becquerel Calibration Factor)

Prior to use QSPECT, BCF needs to be defined. This can be done by scanning a small syringe of known radioactivity, typically supplied from radio-pharmaceutical companies.

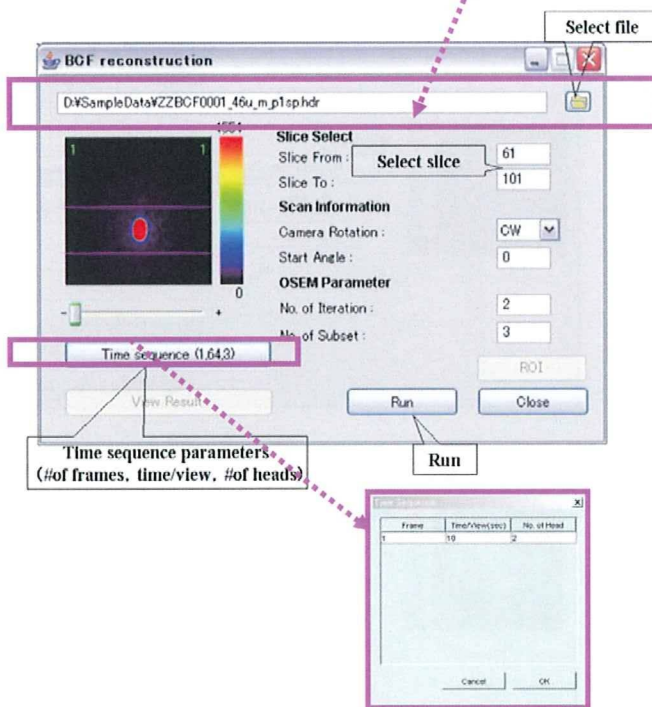


To define BCF in QSPECT, select BCF reconstruction menu in Settings, and do reconstruction for a single-slice projection that covers the whole activity. BCF can then be calculated as the true radioactivity over the pixel counts of the reconstructed image.

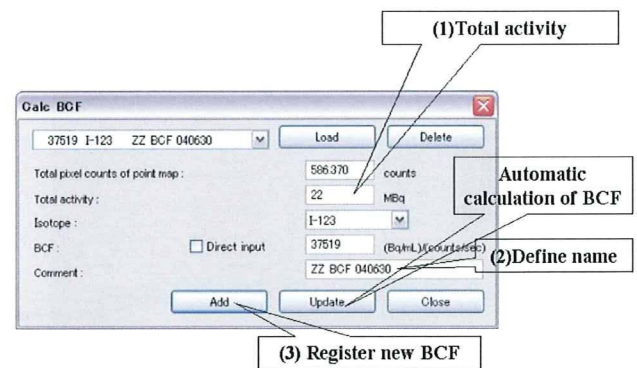
Settings→BCF reconstruction



Hot Source Projection Data



Columns in Time sequence need to be filled as:
 The number of frames (1 if single time frame)
 Acquisition time (sec)/View
 Number of heads (SPECT cameras)



$$BCF((Bq/mL)/(counts/sec)):$$

$$BCF = \frac{\text{Time activity (MBq)}}{\text{(Total pixel count of point map (counts))}}$$

b) TDCS parameter for ¹²³I

TDCS scatter correction technique requires a previously-determined attenuation-to-scatter fraction table for each isotope. Previous studies demonstrated that collimator dependency of this table was minimal, and virtually the same table can be applied to most isotopes such as ^{99m}Tc and ²⁰¹Tl. ¹²³I has a unique problem associated with the penetration of high-energy photons which cause large background over the whole field-of-view. TDCS algorithm could include empirically this fraction by defining a constant background in the attenuation-to-scatter fraction table. However, this constant significantly depends on the design parameters of the collimator. The QSPECT program includes several tables for most commercially available collimators. Chose appropriate TDCS parameter values in Settings, if one wish to use QSPECT for ¹²³I compounds. This is needed only for ¹²³I, but the same parameter

sets can practically be applied to other isotopes such as ^{201}Tl and $^{99\text{m}}\text{Tc}$.

c) Data Directory

Default directories can be set by selecting Options in Settings.

2. Image Reconstruction

To run:

QSPECT>QSPECT Reconstruction

1. Select Emission Projection File:

QSPECT can load multiple image files to reconstruct images using a common mu-map data.



4. OSEM Parameter

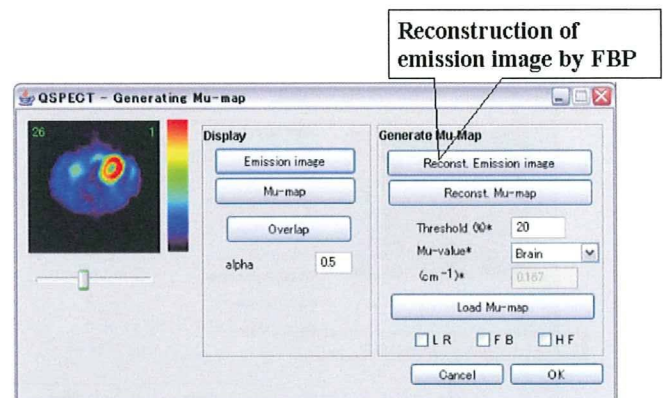
No. of Iteration:

No. of Subset:

Attenuation Map File:

5. Generating Mu-map

This menu can be used to define previously-determined attenuation mu map. The mu map can be superimposed to emission images reconstructed without attenuation or scatter correction by FBP, so that the mu map is obtained at the consistent position with emission data.



2. Confirm and set scan information

CCW/CW CW(clockwise) or CCW (counterclockwise)

Start angle 0 or 90 or 180 or -90 only

Head/feet-in

Matrix size (displayed automatically by use of data information)

of frames (displayed automatically by use of data information)

of projections (displayed automatically by use of data information)

Emission isotope (TDCS parameters will automatically defined)

Transmission isotope

BCF value

3. Define reconstruction parameters

Slice From:

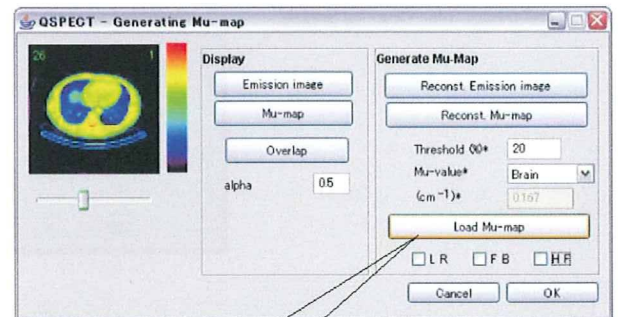
Slice To:

Thickness: unit of pixel

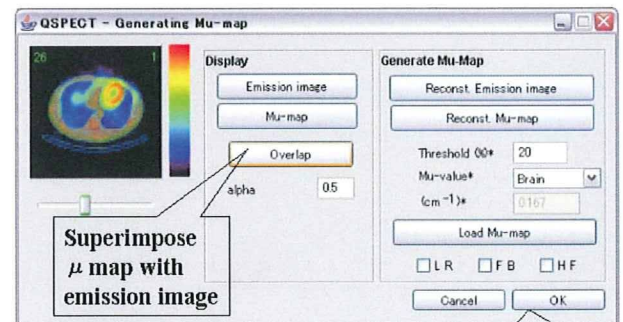
Pitch: unit of pixel

No. of planes (determined automatically)

No. of frame unit of integer



Load existing μ map



Superimpose μ map with emission image

Set mu map for further reconstruction

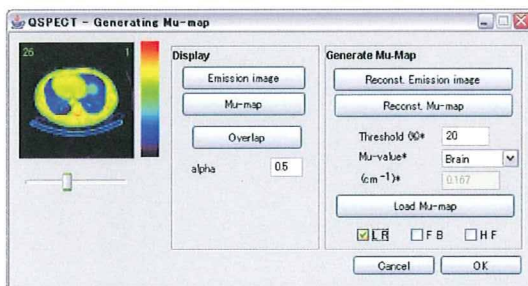
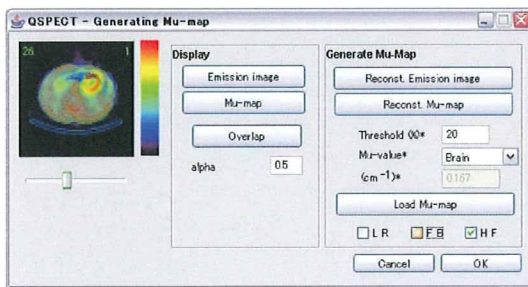
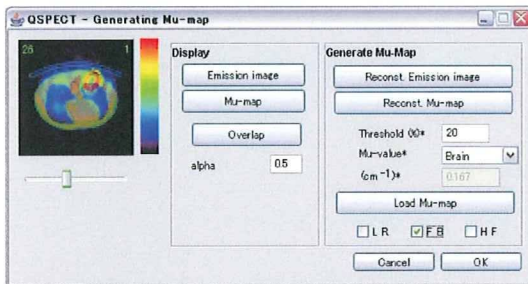
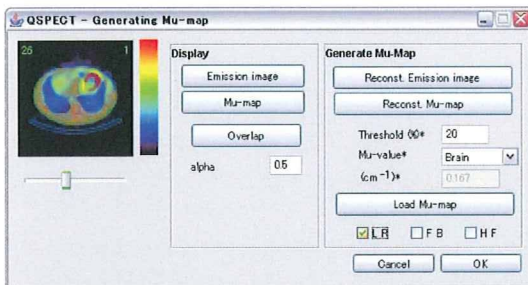
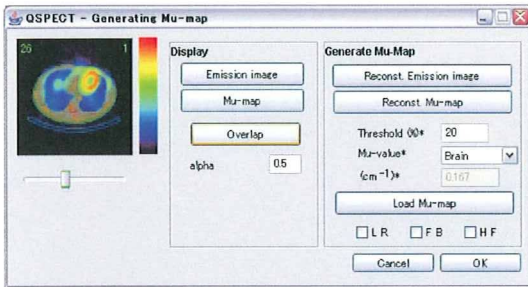
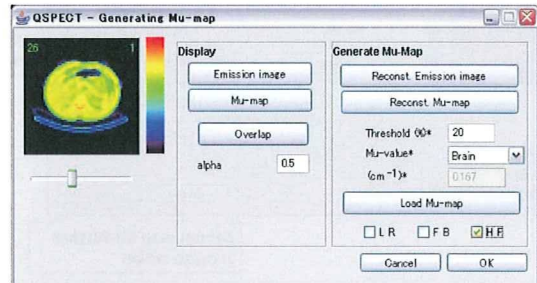
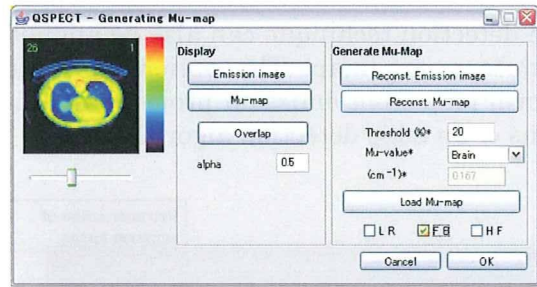
Mu map images can be flipped by selecting LR, FB, and HF switches

LR: Left or Right

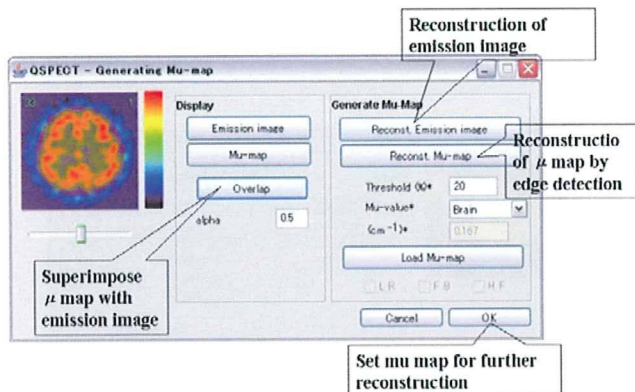
FB: Front or Back

HF: Head or Foot

Multiple columns can be selected, and after finding the suitable direction, click OK. The mu image can be coordinated so as to become consistent with the emission projection data. .



Edge detection technique can also be applied to generate a mu map. This option generate a uniform-map from emission projection data by means of an edge-detection algorithm.



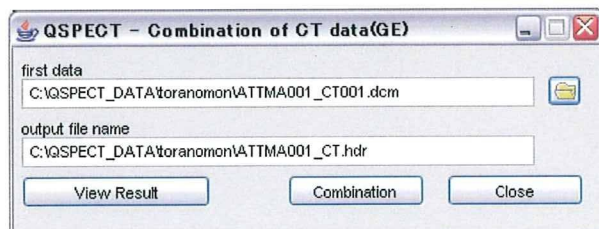
Define optimal threshold(%) for edge detection.
 Define Mu-value suitable for give emission isotop
 and for object (Brain, Phantom or Others)

Mu map defined by separate program could also be loaded in QSPECT as follow.

6. Loading slice-by-slice mu-map files to QSPECT

In case of reading separately defined mu-map in QSPECT, the mu map file should be a single file. If mu maps are given in slice-by-slice as separate files, QSPECT can combine those mu maps into a single file as follows:

Select Settings -> Combination of CT data (GE)



Choose the mu-map file that corresponds to the first slice, and define output file name. Clicking the Combination button generate the single mu map file, and View Result displays the resultant image.

The input file format should be either Dicom or Analyze. Output file is in Analyze format.

6. Reconstruction

Click Run to start QSPECT reconstruction.

Reconstructed image can be displayed by pushing button of "View Results".

Installation

1. Requirements

User interface of the QSPECT program is written in JAVA. QSPECT thus requires JAVA to be installed. JAVA is available from SUN with the following address:

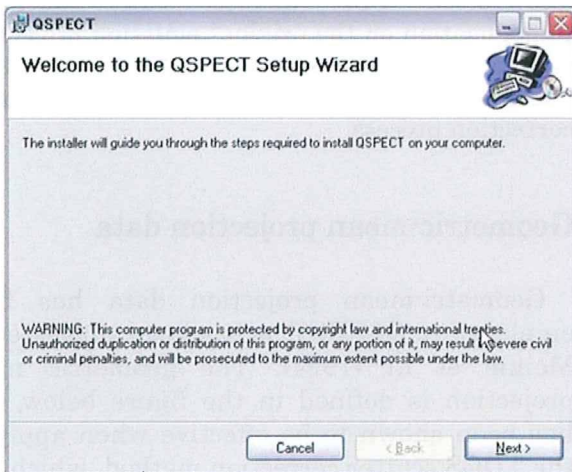
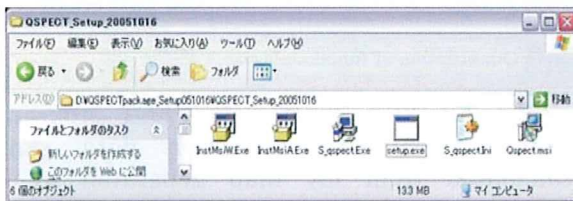
<http://Java.sun.com/products/archive/index.html>

Download J2RE of 1.4.2_0, J2SDK/J2RE -1

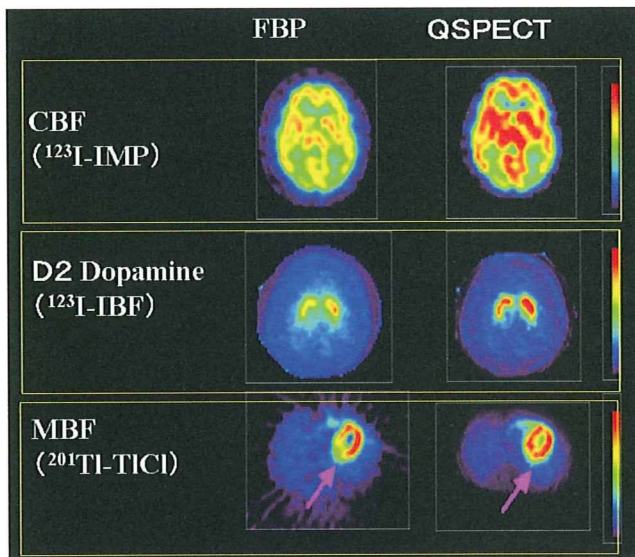
JAVA 1.4.1 or more is needed. Please follow the instruction from SUN.

2. How to install

After installing JAVA, please install QSPECT from the CD:



Example data



Typical examples of QSPECT reconstruction in comparison with Filtered Back Projection technique.

Appendix – Overview of Quantitative SPECT

This section presents a brief overview of quantitative SPECT reconstruction, and background of QSPECT. One of the aims of QSPECT is to improve the SPECT reconstruction so as to make the kinetic analysis possible, for the projection data obtained from clinical SPECT scanners. It is essential that the regional radioactivity concentration is quantified accurately at every temporal period in each myocardial tissue element, which mandates accurate correction for the effects of attenuation and scatter occurring in the body (see in Figure A1).

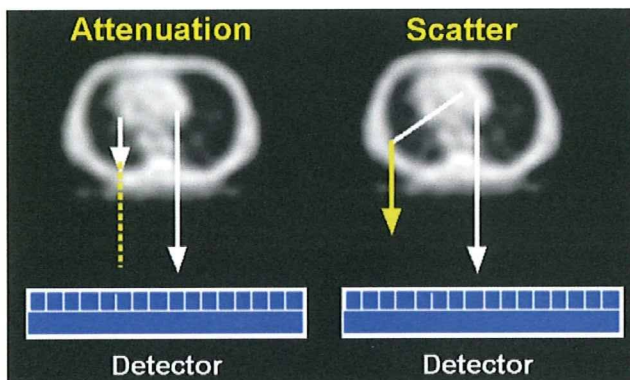


Figure A1. Attenuation and scatter in SPECT

Previous SPECT reconstruction has neglected those two error sources. In addition, Filtered-Back Projection technique has often been applied to truncated data, typically

obtained for limited projection angles such as 180 degree in stead of 360 degree. Due to these factors, SPECT has been considered not to provide quantitative images which are proportional to true radioactivity distributions in the body.

QSPECT reconstruction program has been developed so as to reconstruct true radioactivity concentration in vivo. Accurate correction has been achieved both for attenuation and scatter. Flow chart of QSPECT reconstruction program is shown in Figure A2.

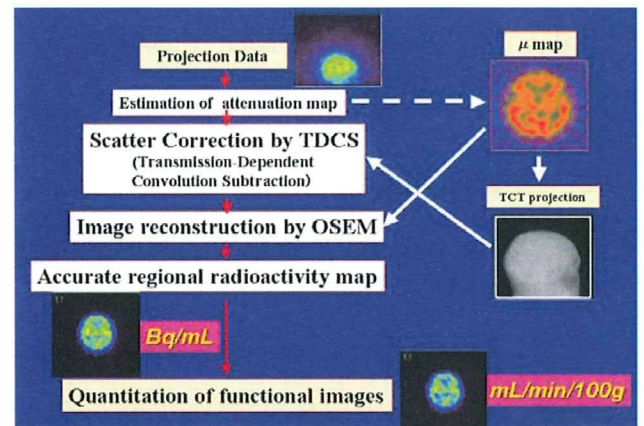


Figure A2. Flow chart of QSPECT program for brain. Attenuation projection data can be calculated from μ map generated by edge detection procedures on scatter-attenuation uncorrected FBP images. After scatter compensation on the original emission projection, true activity distribution can be reconstructed using OSEM program including attenuation correction process.

Geometric-mean projection data

Geometric-mean projection data has been employed in QSPECT as has been suggested by Meikle et al (1994). The geometric mean projection is defined in the figure below, and has been shown to be effective when applying the TDCS scatter correction method, which will be discussed later.

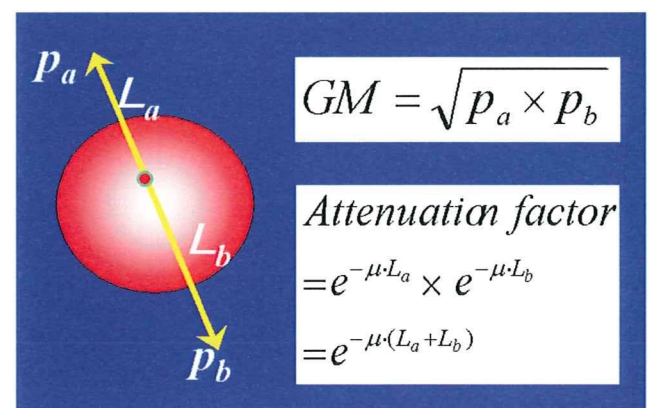


Figure A3. Geometric-mean (GM) projection. GM is a square-root of a product of opposed projection counts.

Attenuation mu-map assessment

Attenuation occurs when photons emitted by the radio-tracer in the patient are absorbed by intervening tissue between the detector and the emission of the photon. The fraction of photons absorbed depends both on the thickness and density of the intervening tissue. Because of the heterogeneous attenuating tissues in the thorax region (i.e. lung, soft tissue, bone etc.), uniform attenuation can not be assumed and measurement of the attenuation information is required. The required distribution of the attenuation factors (μ -maps) can be measured using an external radioactive source attached to an existing SPECT camera. Various geometrical transmission source configurations, ranging from plane sources to scanning line sources and line sources at the focus of fan beam collimators, have been implemented (**Figure A4**). The relative merits of the various configurations have been reviewed by other investigators such as King et al (1995). While all these configurations provide attenuation correction sufficient for qualitative image interpretation, quantitative accuracy is not guaranteed unless the following considerations are taken into account. It is of importance in the design of the transmission system to minimize scattered photons in the transmission projections. Scatter in the transmission projections causes an underestimation of attenuation coefficients and hence undercorrection for attenuation, particularly of deep structures. This makes uncollimated plane sources unsuitable for quantitative attenuation correction, unless the transmission projections are scatter corrected. Collimated scanning line sources with parallel beam collimators on the detectors inherently provide low transmission scatter. An electronic window, synchronized to the mechanical motion of the line source, can in addition minimize the crosstalk of emission counts into the transmission projections when transmission is performed post injection of the emission tracer (18). Transmission projection scatter for symmetrical or asymmetrical fan-beam collimator systems is also intrinsically low, if the transmission source is placed at the focal line of the collimator, and thus physical (or electrical) collimation of the transmission source is not required. However, truncation of

the transmission measurement becomes a source of errors for symmetrical fan-beam collimators and cross-talk from emission activity is substantially higher than for the scanning line source configuration.

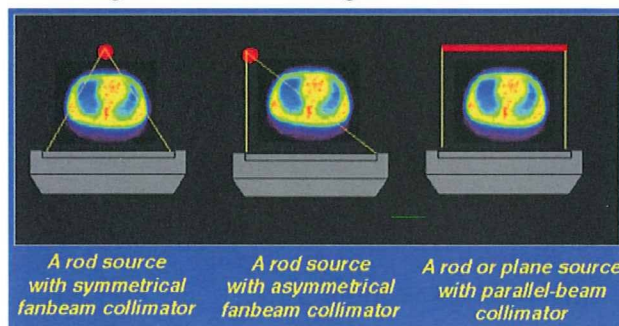


Figure A4. Typical configuration of transmission system in clinical SPECT scanners

Virtually any radioisotopes can be used in the transmission scan, as long as the energy of the transmission source is not vastly different from that of the emission acquisition. Several radioisotopes have been employed for this purpose including ^{153}Gd (97 keV, 103 keV), $^{99\text{m}}\text{Tc}$ (140 keV), ^{241}Am (59 keV), ^{57}Co (122 keV). Due to the energy dependence of the attenuation factors (in addition to a small dependency on the atomic number of the attenuating material), a simple scaling of μ maps is required if the emission isotope energy is different from the transmission energy. For instance, if the transmission scan for a ^{201}Tl myocardial study is performed using $^{99\text{m}}\text{Tc}$, the μ maps from the $^{99\text{m}}\text{Tc}$ transmission scan are multiplied by a factor of (0.194/0.155) to provide the μ maps for ^{201}Tl , where 0.194 is the theoretical (narrow-beam) μ value for ^{201}Tl (34 % window on 77 keV) and 0.155 that for $^{99\text{m}}\text{Tc}$ (20% window on 140 keV). This approach has been shown to be valid over the limited range of densities in the thorax.

Alternative approach is based on separate assessment by means of X-ray CT or MRI (**Figure A5**). In case X-ray CT is used, the μ map needs to be scaled in order to correspond to that for emission isotope. Since energy for general X-ray CT scanner is lower, simple scaling may not be used. Segmentation and scaling for each element are often employed for providing μ map that corresponds to the emission isotope. Similarly, MRI images may be of use to generate μ maps, but require segmentation and scaling procedures to provide quantitative μ images that correspond to the emission data set.

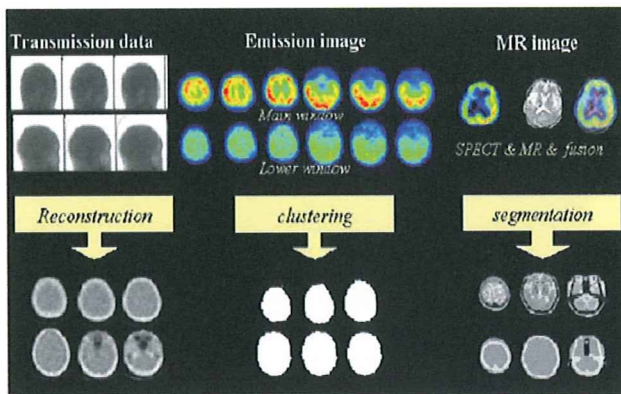


Figure A5. Three typical procedures for generating mu maps.

Reconstruction algorithm used for attenuation correction

Because of simplicity and speed, the filtered-backprojection (FBP) algorithm is generally employed in clinical SPECT studies. Although FBP has been successful in X-ray CT and provides accurate reconstructions in PET, it is not ideal for quantitative SPECT reconstruction. While a range of attenuation correction algorithms have been proposed for FBP reconstruction, these tend not to be exact for non-uniform attenuation regions, such as the thorax. The attenuation effects can be readily included into statistical reconstruction algorithms such as maximum likelihood-expectation maximization (ML-EM), as shown in Figure A6, and this approach potentially provides a more accurate correction for attenuation. ML-EM's major disadvantage of prohibitively long reconstruction time has been largely overcome by increased power of current generation nuclear medicine computers and the introduction of accelerated algorithms. Of the acceleration techniques, the ordered-subset (OS) approach has been shown to be one of the most effective, as this technique provides stable and similar solutions to standard ML-EM, and typically reduces computation time by an order of magnitude by working on subsets of projections at a time. This eliminates the main disadvantage of standard ML-EM and makes OS-EM the method of choice for clinical quantitative SPECT studies. QSPECT program therefore employs the OSEM approach.

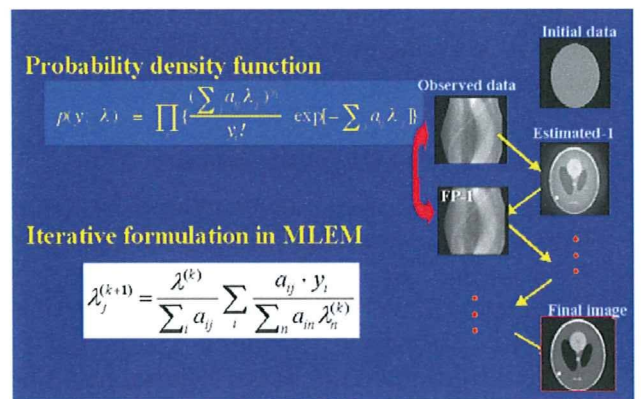


Figure A6. Iterative reconstruction in QSPECT by means of OSEM approach.

Scatter correction

For many years, attenuation was considered the main source of artifacts in myocardial SPECT studies and efforts have concentrated on accurate attenuation correction. More recently, it has been demonstrated that scatter not only contributes to loss of contrast, but also affects quantitative accuracy, and application of attenuation correction without scatter correction can introduce additional artifacts.

The QSPECT program employs a Transmission-Dependent Convolution Subtraction (TDCS) Method as a scatter correction. This algorithm is essentially based on the physical fact that the scatter fraction is a function of attenuation factor, and the greater attenuation, the larger amount of scatter in the projection data. Example procedure of TDCS is demonstrated for brain study in the Figure A7.

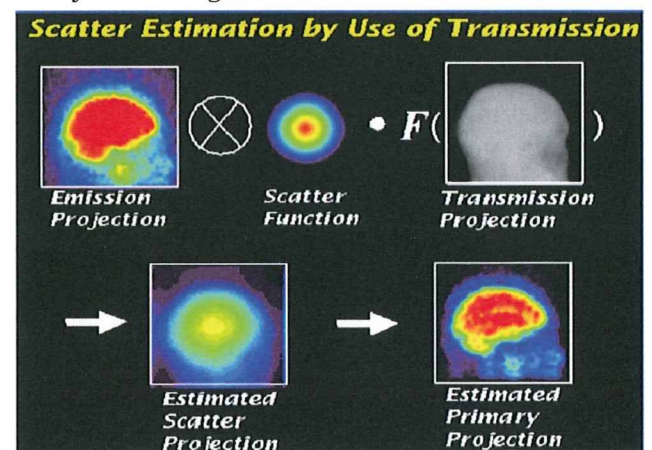


Figure A7. Scatter estimation by use of transmission data in TDCS.

A number of scatter correction techniques have been proposed. These include techniques based on using two or three windows (TEW), which derive scatter from relative counts in the

auxiliary energy windows. Some improvement in accuracy may be achieved by using a larger number of windows or pixel by pixel energy spectra. The relative merits of a range of energy window techniques have recently been compared by Buvat et al (1995). Convolution subtraction techniques estimate the scatter component by convolving the images with a scatter function, but require the assumption of a constant scatter fraction. Assuming a constant, spatially invariant scatter fraction is clearly not applicable in heterogeneous tissues density regions, such as encountered in the thorax. Convolution subtraction scatter correction has thus been extended by Meikle et al (1994) to estimate pixel by pixel scatter fractions from the transmission data and by the work of Ljungberg et al (1991) who used Monte Carlo techniques to calculate the required spatially variant scatter functions and fractions. Appropriate scatter functions and models can obviously also be directly included in the model of iterative reconstruction algorithms such as ML-EM.

Of the energy window based techniques, the TEW method has been shown to achieve reasonable quantitative accuracy under a number of imaging conditions. Although only a limited number of studies have focused on the thorax region, TEW has the advantage that it can be readily implemented on current generation gamma cameras and does not require careful instrument and patient dependent calibration. One potential disadvantage of energy window based techniques for dynamic SPECT is the increased noise introduced by the scatter estimation derived from relatively small energy windows. Convolution subtraction techniques are less likely to suffer from this problem due to the heavy smoothing introduced into the scatter estimate by the convolution with the scatter function. Transmission dependent convolution subtraction (TDCS) has been shown to potentially provide accurate scatter correction for myocardial SPECT and is computationally considerably less intensive than the Monte Carlo techniques. We thus systematically compared TEW with a modified TDCS for scatter correction in the thorax both for ^{99m}Tc (Narita et al., 1996) and ^{201}Tl (Narita et al., 1997) using Monte Carlo simulations and phantom studies, with a specific aim of applying them to dynamic SPECT.

The next 2 Figures show results from a Monte Carlo simulation study which compared TEW and TDCS scatter correction techniques.

For the first Figure, a homogenous ring of myocardium containing ^{201}Tl was simulated in a thorax derived from a clinical transmission study. It can be seen that TDCS provides accurate scatter correction, while TEW overcorrects for scatter in the anterior region, causing an apparent defect. Monte Carlo simulation results for the more realistic MCAT phantom are shown in the next Figure. Again the image scatter corrected with TDCS agreed better with the ideal image than that corrected by TEW. Accuracy in the myocardium for the TDCS corrected image was 4.3%, compared to -16.2% for the TEW corrected image. The figure also clearly demonstrates the superior noise properties of TDCS over TEW. We concluded from these studies that TDCS is a practical method for scatter correcting dynamic SPECT data, providing both improved accuracy and less noise than TEW.

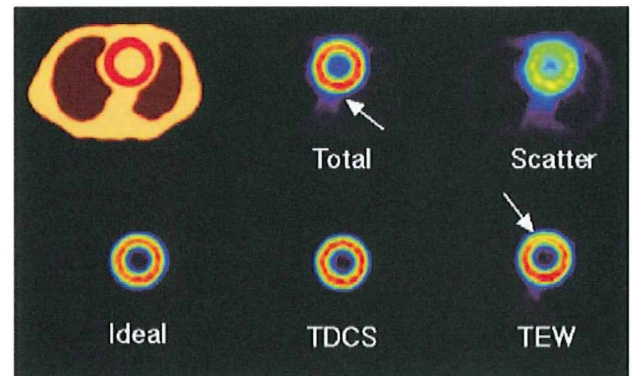


Figure A8. Results of monte Carlo simulation for chest phantom. ^{201}Tl is filled in a homogeneous ring area in thorax geometry, and reconstructed images are compared for two scatter correction techniques of TDCS and TEW. TDCS provided better homogeneity than TEW, which is attributed to the projection-angle dependency of photon energy of the scatter. Greater amount of scatter is subtracted in the anterior wall side, attributed to the large angle scatter.

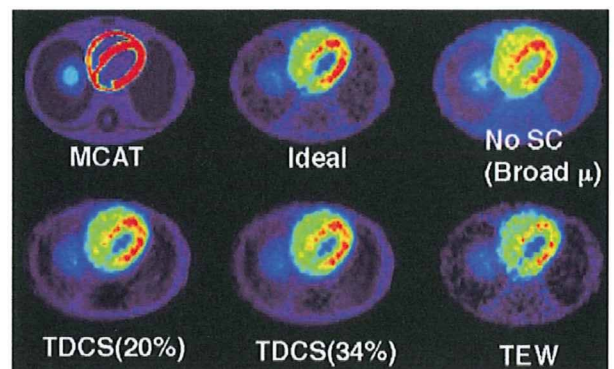


Figure A9. Results of Monte Carlo simulation obtained from MCAT phantom geometry. In this simulation propagation of statistical noise

was compared between TDCS and TEW, and demonstrated that TDCS better statistical property as compared with TEW.

Validity of radioactivity quantitation

The validity of QSPECT is demonstrated in **Figure A10**, in which reconstructed μ and ^{201}Tl images are shown for three cylindrical phantoms with different diameters as well as a ring phantom located in heterogeneous attenuation material. In this experiment, the transmission scan was performed using a physically-collimated rod source system filled with approximately 1 GBq of $^{99\text{m}}\text{Tc}$ and fitted to a parallel-beam collimated gamma camera. The scatter in the emission projection data was subtracted by the TDCS method, and the images were reconstructed with OS-EM and attenuation correction. Each phantom contained the same concentration of ^{201}Tl (approximately 0.2 $\mu\text{Ci/ml}$ or 7.4 kBq/ml). Pixel counts in the reconstructed images are homogeneous, with no systematic differences related to cylindrical phantom size. The homogeneous radioactivity concentration in the ring was also well reproduced in the reconstructed images, despite heterogeneous attenuation and scatter in the phantom, confirming the validity of our approach for heterogeneous regions. It should, however, be noted that the estimated regional radioactivity concentration in the ring phantom was significantly smaller compared with that in the uniform cylindrical phantoms, although the ring phantom contained the same radioactivity concentration as the other phantoms. This is due to the partial volume effect discussed above, which has not been corrected for in these reconstructions. It is also worth noting that depth dependent resolution effects, which should cause non-uniformity in the reconstructed ring, are not evident in this experiment. This is most likely due to the fact that geometric mean data were reconstructed (inherently generated by TDCS scatter correction), which reduces the effects of depth dependent resolution.

The reconstructed μ images were homogeneous for all phantoms, and yielded a quantitative μ value of 0.154 cm^{-1} for $^{99\text{m}}\text{Tc}$, which is in good agreement with the theoretically expected value for 140 keV photons in water. This further confirms the validity of quantitative μ map measurement using the transmission system.

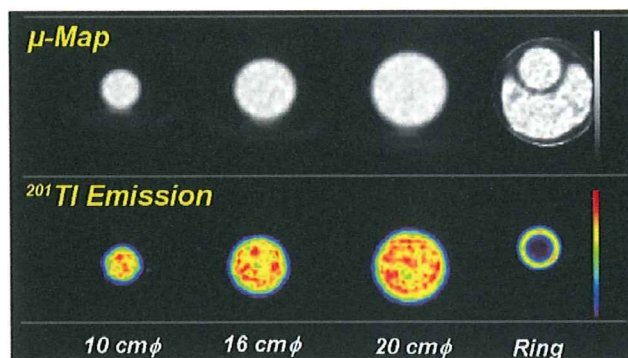


Figure A10. Results of cylindrical phantom experiments. The left three phantoms are uniform cylinders with different diameters filled with ^{201}Tl . The right phantom contains ^{201}Tl in the homogeneous ring region.

Another example to validate the QSPECT reconstruction is demonstrated in **Figure A11**, in which ^{201}Tl was filled in a cylindrical and ring areas placed in attenuation materials which simulate thorax. It is obvious that the reconstructed image was not homogeneous in a ring region, neither in a cylinder region, if no correction was applied for attenuation or scatter (NoAC, NoSC). Homogeneity was improved significantly by attenuation correction alone (AC, NoSC), but still limited in a ring region. Best reconstruction was confirmed when both corrections are applied for attenuation and scatter (AC, SC).

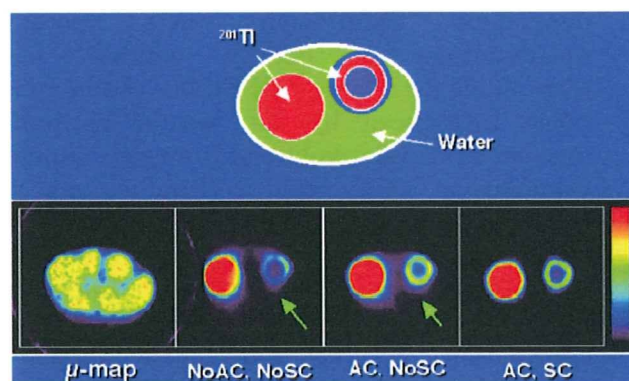


Figure A11. Results from a chest phantom experiment with ^{201}Tl in myocardial ring and cylindrical liver regions.

Clinical study

Figure A12 shows representative ^{201}Tl myocardial slices, at the mid-ventricular level, from a normal volunteer using a conventional 2-head gamma camera (Toshiba GCA-7200A, Tokyo, Japan), which demonstrate the effects of attenuation and scatter corrections. Without attenuation correction, a large defect is

apparent in the posterior wall for both the 180 and 360 degree reconstructions. This is attributed to the larger attenuation of photons emitted from deep structures. Attenuation correction without scatter correction overcompensates the posterior wall counts, causing an apparent defect in the anterior wall. After correcting for both attenuation and scatter, the nearly homogeneous counts expected for a normal volunteer, are obtained along the myocardial wall. It is clear from these images that both attenuation and scatter corrections are essential in order to calculate images for quantitative assessment.

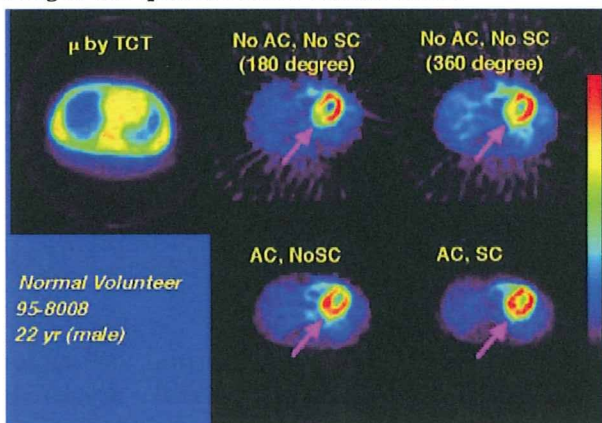


Figure A12. Results from a normal volunteer study with ^{201}Tl .

Figure A13 shows sequential images following intra-venous injection of ^{201}Tl (111 MBq) obtained from the same normal volunteer using the same equipment. In this measurement, the detectors were continuously rotated to provide a complete SPECT projection data set every 15 seconds. The projection data sets were summed into 10 x 2 min frames, followed by 5 x 4 min frames and finally 9 x 5 min frames for a total acquisition time of approximately 85 min. The images were reconstructed with our quantitative SPECT approach outlined above. These images demonstrate that our quantitative approach is also applicable to dynamic SPECT studies, without undue amplification of noise. These dynamic images form the prerequisite to analyze the kinetics of ^{201}Tl in each myocardial region, and thus quantitative estimates of the physiologically-meaningful parameters can be performed based on a mathematical compartmental model. Regional myocardial blood flow and distribution volume for ^{201}Tl can also be calculated according to a compartmental model analysis as has been successfully done in PET. The influx rate constant, namely K_1 represent the absolute regional myocardial blood flow, and V_d denotes

the ability of retaining ^{201}Tl in tissue relative to the blood (see below).

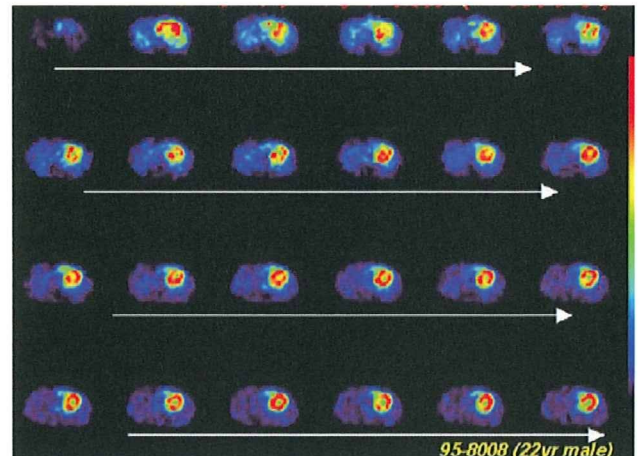


Figure A13. Sequential images of myocardial region following i.v. ^{201}Tl in a normal volunteer.

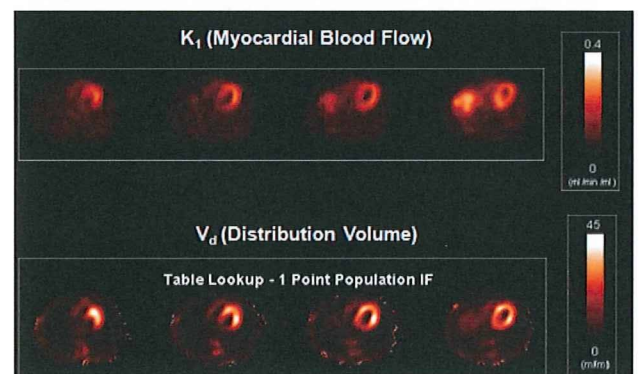
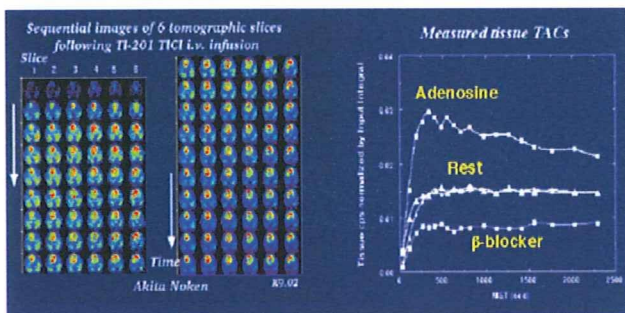


Figure A14. Quantitative mapping of absolute myocardial blood flow (K_1 mL/min/mL) and regional volume of distribution (mL/mL) for ^{201}Tl obtained from a dynamic SPECT scan on a normal volunteer.

One of the prerequisites for kinetic analysis is that quantitative SPECT provides reconstructed counts which are directly proportional to the activity concentration in the tissue. Thus an increase in activity concentration due to, for example, increased blood flow should cause a corresponding increase in the reconstructed counts. **Figure A15** plots regional time-activity curves obtained from a series of dog experiments at rest ($n=2$) and during constant intravenous administration of adenosine ($n=1$) and beta-blocker ($n=1$). It is apparent that the regional radioactivity curves correspond well with the physiological conditions introduced by the drug administration. When flow is increased by adenosine infusion, the quantitative SPECT reconstruction correctly identifies increased absolute ^{201}Tl radioactivity accumulation rate as well as increased washout rate. During beta-blocker infusion, the ^{201}Tl uptake is

suppressed and clearance rate is also reduced. As shown **Figure A16**, the MBF values calculated with the compartment model analysis agreed well with those determined from the in vitro microsphere experiment in a canine model for a physiologically wide range. The approach has further been validated in a split-dose protocol on pigs, as shown in **Figure A17**. These findings strongly support the use of clinical SPECT systems for absolute quantitation of MBF at rest and even the coronary flow reserve in man.



curves at rest (n=2), during adenosine infusion (n=1), and after beta-blocker administration (n=1).

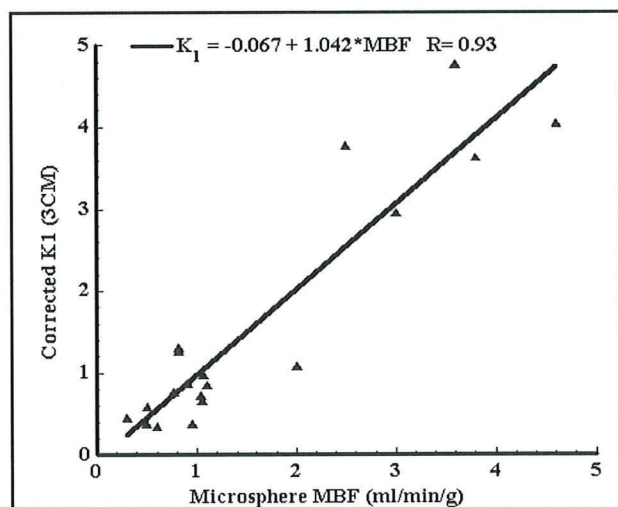


Figure A16. Quantitative mapping of absolute myocardial blood flow (K_1 mL/min/mL) and regional

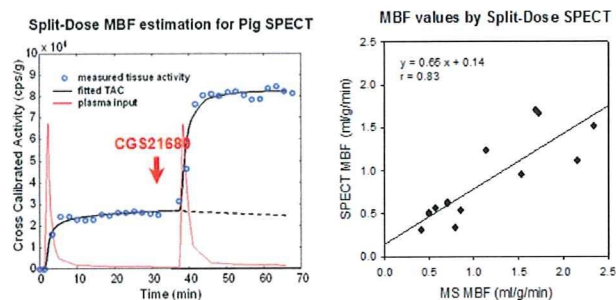


Figure A17. Quantitative mapping of absolute myocardial blood flow (K_1 mL/min/mL) and regional

Potential of Kinetic analysis

^{201}Tl is well recognized as a potassium analogue, and its kinetics have been extensively investigated. Due to a high transcapillary extraction fraction, it is rapidly accumulated into the myocardial tissue, and initial regional uptake of this tracer predominantly reflects regional blood flow. ^{201}Tl clears rapidly from arterial blood, reducing delivery of tracer to the myocardium. When an equilibrium between myocardium and blood ^{201}Tl concentration is reached, the myocardial concentration of ^{201}Tl no longer reflects flow, but the myocardium's ability to retain ^{201}Tl and is related to the number of myocytes with maintained membrane potential in a given volume of myocardium. This equilibrium uptake is related to the volume of distribution (V_d [ml/ml]) parameter used in kinetic modeling. Thus behavior of ^{201}Tl varied largely dependent on physiologic/pathophysiologic status of the myocardium, such as for normal, ischemic and infarcted regions. In normal myocardium, there is rapid initial uptake reflecting normal flow, followed by slow clearance towards equilibrium. For ischemic myocardium with maintained cell potential, initial uptake is low due to low flow, and uptake continues towards the same equilibrium as normal myocardium (redistribution). In infarcted areas, reduced flow causes initial reduced uptake and loss of cell membrane potential causes loss of ability to retain ^{201}Tl and increased clearance rate. Thus delayed images at 3-4 hours and up to 24 hours are used clinically to differentiate reduced flow, but viable (normal V_d) areas from infarcted regions which also have reduced flow, but also reduced V_d . It should be noted that, given the slow kinetics of ^{201}Tl , equilibrium is not necessarily achieved within 3-4 hours, thus the delayed images contain a mixture of flow and V_d information. Images at 24 hours better reflect V_d , but suffer from poor counting statistics and the inconvenience of the patient having to attend on another day. Thus one of the main attractions of kinetic analysis of dynamic data is its potential to separate flow and V_d components, providing true flow and true equilibrium (V_d) images. Quantitative dynamic SPECT reconstruction should have high potential to extract such physiologic parameters.

Conclusion

Theoretical background, validation and potential application of QSPECT have been described. Accurate quantitation of regional radioactivity concentration is feasible in SPECT using appropriate reconstruction, attenuation and scatter correction techniques, as has been demonstrated by our Monte Carlo simulations and phantom studies. The increased sensitivity of multi-head cameras and improvements in reconstruction algorithms allowed the kinetic analysis to be accurately assessed, making application of a mathematical compartmental model feasible. It has been suggested that SPECT has the potential for absolute quantitation of biophysiological functions noninvasively in clinical studies. The QSPECT program should have a number applicability in clinical research using various SPECT tracers.

<Literatures>

Accuracy and legitimacy for QSPECT:

Iida H, Shoji Y, Sugawara S, Kinoshita T, Tamura Y, Narita Y and Eberl S. Design and Experimental validation of a Quantitative myocardial ^{201}Tl SPECT System. *IEEE Trans Nucl Sci*;46:720-726,1999.

Iida H, Narita Y, Kado H, Kashikura A, Sugawara S, Shoji Y, Kinoshita T, Ogawa T, Eberl S. (1998) Effects of scatter and attenuation correction on quantitative assessment of regional cerebral blood flow with SPECT. *J Nucl Med* 39:181-189 (optimized/validated for brain ^{123}I)

Effectiveness and application of QSPECT:

Iida H and Eberl S. Quantitative assessment of regional myocardial blood flow with thallium-201 and SPECT. *J Nucl Cardiol*;5:313-31,1998.

Scatter Correction:

Meikle SR, Hutton BF, Bailey DL. (1994) A transmission-dependent method for scatter correction in SPECT. *J Nucl Med* 35:360-367 (originally proposed)

Narita Y, Eberl S, Iida H, Hutton BF, Braun M, Nakamura T and Bautovich G. Monte Carlo

and experimental evaluation of accuracy and noise properties of two scatter correction methods for SPECT. *Phys Med Biol*;41:2481-96,1996 (optimized/validated for cardiac $^{99\text{m}}\text{Tc}$)

Narita Y, Iida H, Eberl S and Nakamura T. Monte Carlo evaluation of accuracy and noise properties of two scatter correction methods for ^{201}Tl cardiac SPECT. *IEEE Trans Nucl Sci*;44:2465-2472,1997. (optimized/validated for cardiac ^{201}Tl)

Ito H, Iida H, Kinoshita T, Hatazawa J, Okudera T and Uemura K. Effects of scatter correction on regional distribution of cerebral blood flow using I-123-IMP and SPECT. *Ann Nucl Med*;13:331-6,1999.

Kim KM, Watabe H, Shidahara M, Ishida Y and Iida H. SPECT Collimator Dependency of Scatter and Validation of Transmission-Dependent Scatter Compensation Methodologies. *IEEE Trans Med Image*;48:689-696,2001.(collimator dependency for ^{123}I)

Shidahara M, Watabe H, Kim KM, Hachiya T, Sayama I, Kanno I and Iida H. Impact of attenuation and scatter correction in SPECT for Quantification of cerebral blood flow using $^{99\text{m}}\text{Tc}$ -Ethyl cystenate dimer. *IEEE Trans Nucl Sci*;49:5-11,2002.

Kim KM, Varrone A, Watabe H, Shidahara M, Fujita H, Innis RB and Iida H. Contribution of scatter and attenuation compensation to SPECT images of non-uniformly distributed brain activities. *J Nucl Med*;44:512-519,2003.

Ljungberg M, Strand S-E. Attenuation and scatter correction in SPECT for sources in a nonhomogeneous object: a Monte Carlo study. *J Nucl Med* 1991; 32: 1278-1284.

Ichihara T, Ogawa K, Motomura N, Kubo A, Hashimoto S. Compton scatter compensation using the triple-energy window method for single- and dual-isotope SPECT. *J Nucl Med* 1993; 34: 2216-2221.

Buvat I, Rodriguez-Villafuerte M, Todd-Pokropek A, Benali H, Di Paolo R. Comparative assessment of nine scatter correction methods based on spectral analysis using Monte Carlo simulations. *J Nucl Med* 1995; 36: 1476-1488.

Larsson A, Johansson L. Transmission-Dependent Convolution Subtraction of $^{99\text{m}}\text{Tc}$ -

HMPAO rCBF SPECT- A Monte Carlo Study. IEEE T Nucl Sci, 52(1):231-237, 2005

Larsson A, Johansson L. Scatter-to-primary based scatter fractions for transmission-dependent convolution subtraction of SPECT images. Phys. Med. Biol, 48:N323-N328, 2003

M Ljungberg, Larsson A, Johansson L. A New Collimator Simulation in SIMIND based on the Delta-Scattering Technique. Medical Imaging Conference Proceedings, pp: 1-6, 2006

Larsson A, Ljungberg M, Mo SJ, Riklund K, Johansson L. Correction for scatter and septal penetration using convolution subtraction methods and model-based compensation in 123I brain SPECT imaging- a Monte Carlo study. Phys. Med. Biol, 51:5753-5767, 2006

Zaidi H, Koral KF. Scatter modeling and compensation in emission tomography. Eur J Med Mol Imaging 31:761-782, 2004

Ordered-Subset ML-EM:

Hudson HM, Larkin RS. (1994) Accelerated image reconstruction using ordered subsets of projection data. IEEE Trans Med Imaging MI-13:601-609

Geometric mean reconstruction:

Larsson A, Johansson L, Sundstrom T, Ahlstrom KR. A method for attenuation and scatter correction of brain SPECT based on computed tomography images. Nucl Med Commun, 24:411-420, 2003

Attenuation correction review:

King MA, Tsui BMW, Pan T-S. Attenuation compensation for cardiac single-photon emission computed tomographic imaging: Part 1. Impact of attenuation and methods of estimating attenuation maps. J Nucl Cardiol 1995; 2: 513-524.

King MA, Tsui BM, Pan TS, Glick SJ, Soares EJ. Attenuation compensation for cardiac single-photon emission computed tomographic imaging: Part 2. Attenuation compensation algorithms. J Nucl Cardiol 1996; 3: 55-64.

Rosenthal MS, Cullom J, Hawkins W, Moore SC, Tsui BM, Yester M. Quantitative SPECT imaging: a review and recommendations by the Focus Committee of the Society of Nuclear Medicine Computer and Instrumentation Council. J Nucl Med 1995; 36: 1489-1513.

放射線診療部に設置された研究所CT/SPECT装置の

患者情報匿名化サーバーの運用について

国立循環器病センター研究所 先進医工学センター

放射線医学部 部長 飯田秀博

放射線診療部に設置された研究所・放射線医学部部長が導入したシーメンス社製SymbiaT6 (CT/SPECT装置)の使用にあたっては、倫理委員会に承認されたとおり、下記のように運用いただきますようお願いいたします。

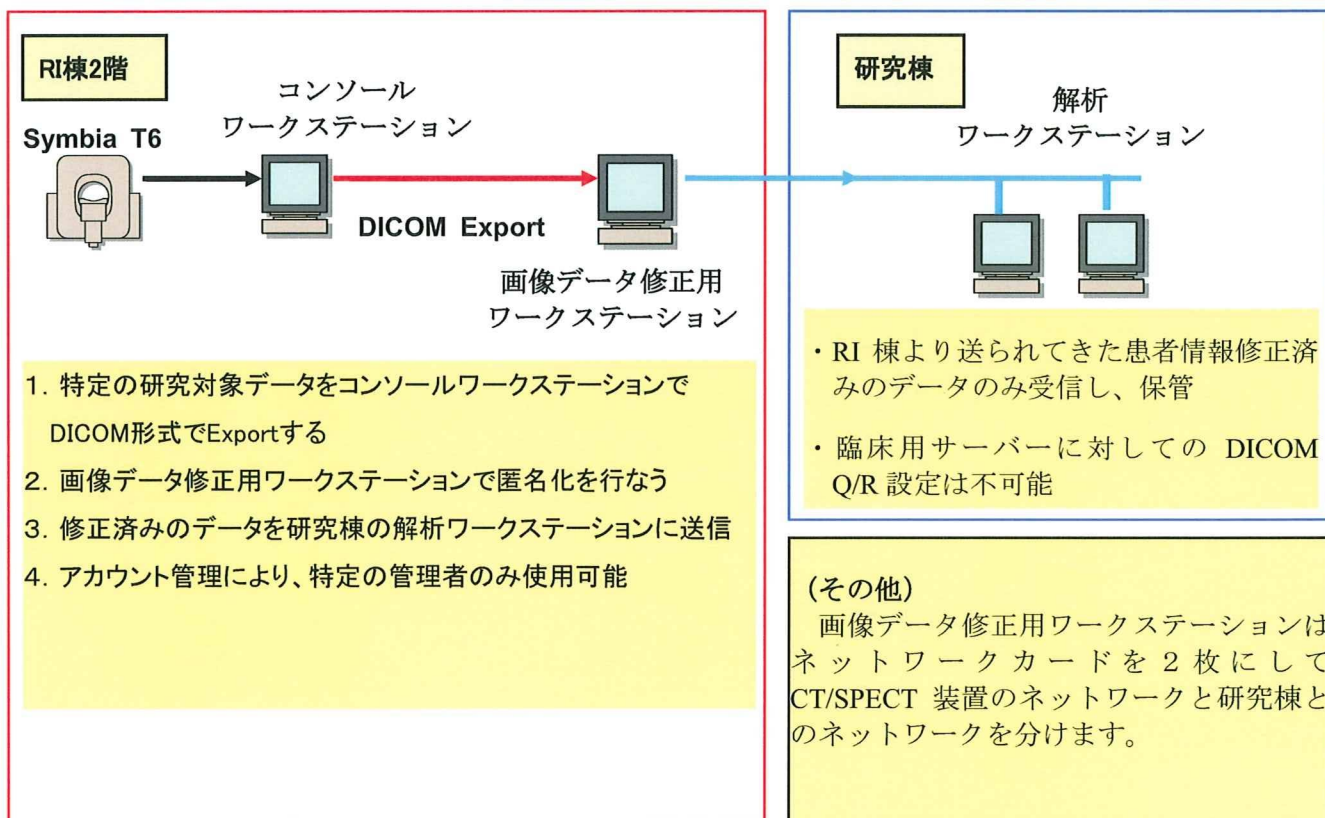
記

【患者情報の研究利用について】

- シーメンス社製 SymbiaT6 (CT/SPECT 装置) にて研究目的に撮像された臨床画像データを研究所サーバーに転送する場合には、画像データに含まれる個人情報の匿名化を行う。この時にデータフォーマットは DICOM とする。倫理委員会により個人情報との連結が承認されている場合には対応表を作成するものとし、個別課題ごとにその責任者が対応表を管理するものとする。

【システムの構築について】

- 以下のシステム構成に基づいて匿名化がなされる。



【匿名化作業の実際について】

- 匿名化作業は、臨床データにおいては放射線診療部部長あるいは RI 検査室医長の責任のもとに、倫理委員会の承認を受けた研究を目的に得られた場合には放射線診療部部長あるいは RI 検査室医長および課題ごとの研究代表者の責任のもとに行われる。実際の作業は上記責任者の任命するものとする。
- 匿名化は、専用サーバーにデータが転送された際に自動的に行われるものとする。ただし、撮像対象が臨床目的に撮像された患者データ以外の場合（倫理委員会にて承認された課題に基づく健常者ボランティア、およびファントムなど）には、匿名化を行う必要はない。

【利用制限について】

- 本ソフトウェアは SPECT 核医学診断の精度向上を目指す研究の支援を目的として提供されるものである。この研究以外での利用を禁じる。

【注意事項】

- 匿名化サーバーの運用に際してはオペレーションガイド（操作マニュアル）に従って慎重に作業を行うものとし、患者情報の保護に十分ご留意する。

匿名化プログラム

本研究事業では、国立循環器病センター研究所が開発した定量的SPECT画像再構成・解析パッケージ(QSPECT)を用いて、Windowsプログラムにおいて個人情報を匿名化するプログラムを作成・整備した。QSPECTパッケージIMP Dual Table ARG法バージョン2.4以降で処理した出力フォルダを指定することで、下記項目について匿名化を行う。

- 患者名
- 患者ID
- 患者誕生日
- 患者年齢
- 患者性別
- 患者住所

QSPECTを用いて解析された画像データは、有害事象の報告、研究事業のプロトコル規約で研究事務局に集約される前に、各データ提供施設にて匿名化処理されることとしている。

(資料 6)では、匿名化プログラムの使用方法について説明する。

——お知らせ——

匿名化プログラム

(QSPECTパッケージ IMP Dual Table ARG法バージョン2.4)

QSPECT DTARG法ご使用の先生方には大変お世話になっております。
この度、パービューザミン注を用いたDual Table ARG法検査においてご使用いただいております
QSPECTパッケージWindowsプログラムにおいて匿名化プログラムを準備しましたので、ご連絡い
たします。よろしく願いいたします。

<内容>

プログラム名: QSPECT Anonymous

QSPECT パッケージ IMP Dual Table ARG 法バージョン 2.4 以降で処理した出力フ
ォルダを指定することで、下記項目について匿名化を行う。

- Patient Name (患者名)
- Patient ID (患者 ID)
- Patient Birthday (患者誕生日)
- Patient Age (患者年齢)
- Patient Sex (患者性別)
- Patient Address (患者住所)

<インストールの方法>

CD をセットすると、自動的にセットアッププログラムが起動します。(自動的に起動し
ない場合は、QSPECT フォルダ内の Setup.exe をダブルクリックしてください。)
デスクトップにあるアイコンをダブルクリックして起動してください。

